

Ruthenium and Rhodium doped sillenite crystals: holographic properties and applications at near-infrared spectral range

Vera Marinova*^a, Ken Y. Hsu^a, Shiuan H. Lin^b, Ren C. Liu^a, Yu H. Lin^a

^a Department of Photonics, National Chiao Tung University, Hsinchu 30010, Taiwan; ^b Department of Electrophysics, National Chiao Tung University, Hsinchu 30010, Taiwan

ABSTRACT

We report an improvement of the response time and near infrared sensitivity of sillenite crystals $\text{Bi}_{12}\text{SiO}_{20}$ (BSO), $\text{Bi}_{12}\text{TiO}_{20}$ (BTO) doped with transition metal ions as Ru and Rh. Real-time holographic recording is performed at 1064 nm at a diffusion regime. By using 532 nm light for pre-excitation, significant operation speed of 20 ms is achieved in case of Rh-doped BTO crystal. Further, a possibility to combine doped sillenite plates with liquid crystal into a organic/inorganic hybrid devices (Liquid Crystal Light Valves) is demonstrated, which opens many prospects for further near infrared photonic applications.

Keywords: photorefractive materials, real-time holography, near-infrared sensitivity, response time, liquid-crystal devices, spatial light modulators

1. INTRODUCTION

Material's properties optimization by doping with transition elements have been a subject of considerable interest for many years. Furthermore, the transition metals ions possesses the ability to exist at different valence states after appropriate light illumination, thus allow to control optically and modulate the properties. In that aspect the near infrared sensitivity improvement and recording speed optimization are of essential importance because of the wide applications of diode lasers in real-time image processing, for non-invasive biomedical objects testing, ...etc. [1,2]. Among inorganic crystals, sillenites $\text{Bi}_{12}\text{MO}_{20}$ ($M=\text{Si}, \text{Ti}, \text{Ge}$) are known as one of the fastest materials for real-time processing and related dynamic applications. Their remarkable photoconductivity and fast response time open many opportunities for dynamic holography and interferometry, optical information processing, and recently for biomedical applications [3-8]. For example, photorefractive digital holographic microscopy applied in microstructured analysis has been demonstrated very recently on $\text{Bi}_{12}\text{TiO}_{20}$ crystal [9]. Moreover, the crystal growth technique is well developed and large samples with excellent optical quality are available.

Recently, a combination of sillenite photorefractive materials with liquid crystals into a hybrid structures opens further possibilities for new optical nonlinear devices as optically addressed spatial light modulators- so called photorefractive liquid crystal light valves (PRLCLVs). In general the light valve is a coherent-to-incoherent image converter, which consists of photoreceptor (photoconductor) and electro-optic material, separated by dielectric mirror. First Aubourg et al. [10] proposed bulk monocrystalline $\text{Bi}_{12}\text{SiO}_{20}$ (BSO) crystal as a photoconductor assembled with a LC molecule into optically addressed transducer. Due to the excellent photoconductivity and high dark resistivity of BSO, when incoherent image is projected into BSO crystal, the light reduces its impedance so the voltage is transferred to the LC layer, resulting in molecular re-orientation. This allows spatial modulation of the amplitude or phase of the incident coherent beam. Later on, Residori et al. [11-13] extended this idea and demonstrated several non-linear applications of LCLV device based on non-doped $\text{Bi}_{12}\text{SiO}_{20}$ at visible spectral range, where the refractive index modulation can be controlled optically or electrically.

Here we present the effect of platinum group doping metals like Ru and Rh on the response time and sensitivity enhancement of BSO and BTO crystals at near infrared spectral range. We show that pre-excitation with an optical energy close to the energy level of the main photorefractive defect center typical for sillenites can improve significantly the response time. Next, a possibility to combine Ru, Rh -doped sillenite crystals with a liquid crystal cell into hybrid organic/inorganic device is demonstrated. The intensity modulation characteristics at near infrared are presented and discussed. Finally, an example of the time evolution of an image on LCVL is demonstrated.

* veramarinova@nctu.edu.tw; vera-marinova@yahoo.com; phone +886 3 5712121 56195; fax +886 3 5725230;

Holography: Advances and Modern Trends III, edited by Miroslav Hrabovský,
John T. Sheridan, Antonio Fimia-Gil, Proc. of SPIE Vol. 8776, 877605 · © 2013
SPIE · CCC code: 0277-786X/13/\$18 · doi: 10.1117/12.2017292

EXPERIMENTAL DETAILS

1.1 Crystal growth and sample preparation

Ru-doped $\text{Bi}_{12}\text{SiO}_{20}$ (BSO:Ru) crystal was grown from stoichiometric solutions by the Czochralski method and Rh-doped $\text{Bi}_{12}\text{TiO}_{20}$ (BTO:Rh) crystal was grown by the Top Seeded Solution Growth Method [14]. The growth processes were conducted in air for BSO:Ru and in mixed atmosphere of 85% air and 15% Ar in case of BTO:Rh. The doping was performed by addition of RuO_2 and RhO_2 oxides into the melt. Dopants concentration in the grown crystals were determined by Atomic Absorption Spectroscopy analysis as $\text{Ru} = 6.1 \times 10^{18} \text{ cm}^{-3}$ and $\text{Rh} = 5.2 \times 10^{18} \text{ cm}^{-3}$, respectively. For holographic experiments, cubes with rectangular dimensions of $10.3 \times 11.4 \times 6.4 \text{ mm}$ for BSO:Ru and $10 \times 7 \times 3.8 \text{ mm}$ for BTO:Rh, both cut along (110), (1-10) and (001) crystallographic directions were prepared. Crystal plates with $15 \times 15 \text{ mm}^2$ lateral size and thickness of 1.2 mm of BSO:Ru and 0.5 mm of BTO:Rh have been optically polished for combination with LC into LCLV devices.

1.2 Real-time holography at 1064 nm.

Holographic recording experiments were performed by two-wave mixing set-up using 1064 nm diode-pumped laser (Fig.1). The intensity of each recording beam was about 100 mW/cm^2 and 26° of the writing angle outside the crystal. The temporal evolution of the recorded grating was probed in real-time by the low power third beam, coming from the same laser source. The intensity of the diffracted light was measured with a Si detector located behind the crystal. For pump excitation cw light coming from Verdi laser source (adjustable intensity) was used for 2-3 min irradiation and IR recording starts immediately after it. Samples were thermally annealed before the experiments.

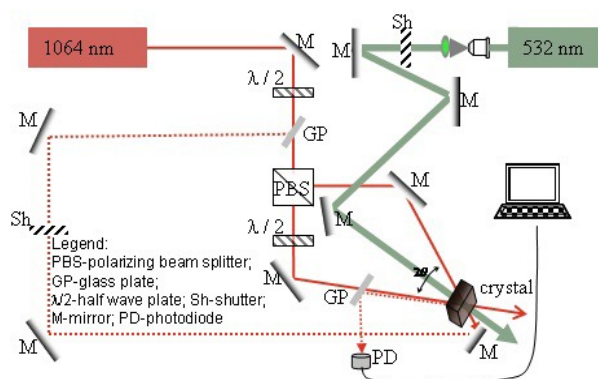


Fig.1 Holographic experimental-set up: recording and readout at real-time using 1064 nm. Green light (532 nm) is used only for pre-excitation.

1.3 Photorefractive liquid crystal light valve

Two PRLCLV devices have been prepared, based on BSO:Ru and BTO:Rh crystal plates. One side of the crystal plate (contacting with the LC) was preliminary coated with indium tin oxide (ITO) and the other side of the crystal plate was coated with a mechanically buffered alignment layer, polyvinyl alcohol (PVA). The liquid crystal type MLC 2070 (thickness of $12 \mu\text{m}$) was sandwiched between the crystal plate and the glass substrate, separated by the teflon spacers. The one side of the glass substrate (contacting with the LC) was also coated with mechanically buffered PVA. A schematic representation of the LCLV device is presented at Fig.2. In order to check the changes of birefringence under the applied voltage and pump intensity, the PRLCLV device was inserted between a pair of crossed polarizers with a liquid crystal director (n) making an angle of 45° with the transmittance axis. Diode-pumped solid state laser operating at 1064 nm was used to pump the intensity change and very weak (few μW) laser beam coming from 790 nm diode laser to monitor the intensity changes. The applied ac voltage with r.m.s amplitude was changed from 2 to 50V at the frequency of 1 kHz

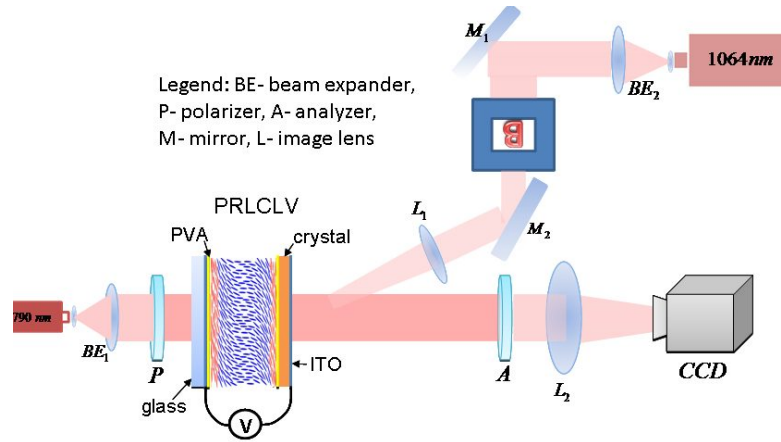


Fig 2. Schematic representation of the LCLV device based on sillenite crystal combined with LC and crossed polarizer experimental set-up to measure the intensity modulation and to demonstrate image illumination.

2. RESULTS AND DISCUSSION

2.1 Real-time holography at near infrared spectral range

Figures 3 and 4 present the real-time holographic recording and erasure behavior of Ru-doped BSO and Rh-doped BTO at 1064 nm (a) without preliminary treatments of the samples and (b) after green light pre-excitation. Both samples

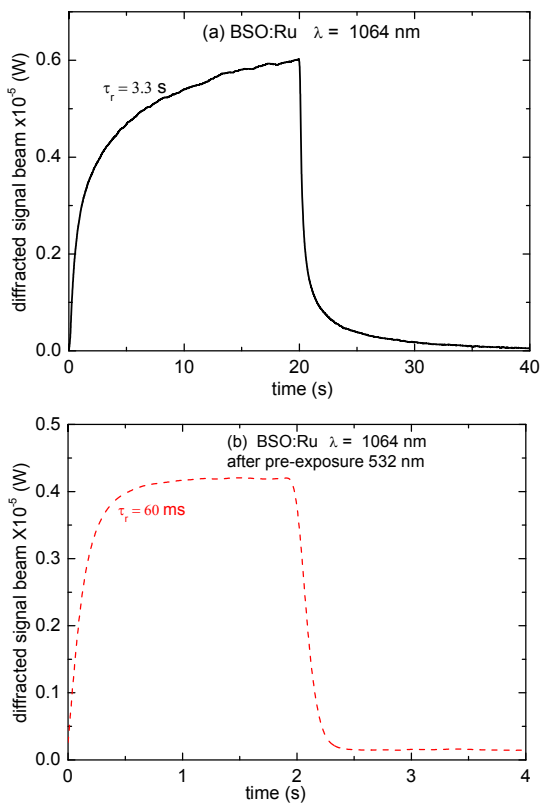


Fig.3. Recording and erasure behaviour of BSO:Ru at 1064 nm in real –time: (a) without any preliminary treatment and (b) after 532 nm pre-excitation with $I = 250 \text{ mW/cm}^2$

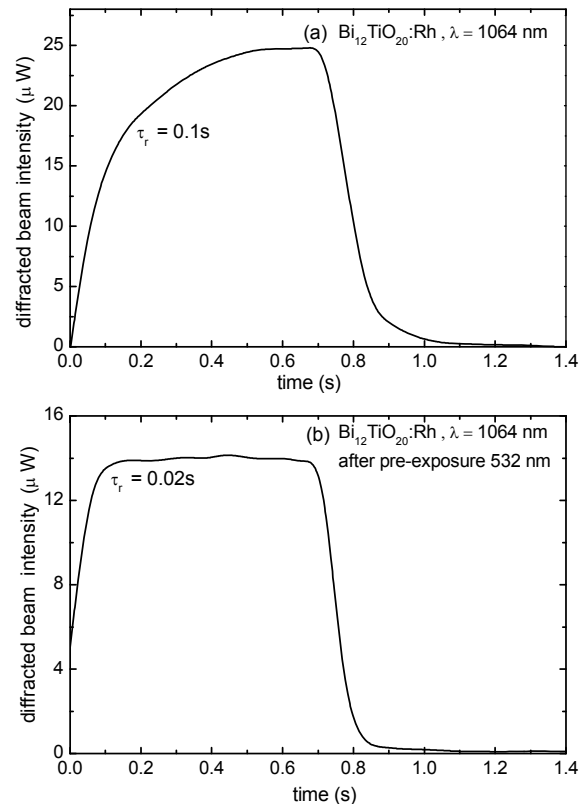


Fig.4. Recording and erasure behaviour of BTO:Rh at 1064 nm in real –time: (a) without any preliminary treatment and (b) after 532 nm pre-excitation with $I = 50 \text{ mW/cm}^2$

show fast exponential rise and decay, with a response time of 0.1s in case of BTO:Rh (see Fig. 4(a)). Once the samples are pre-illuminated with 523 nm green light (with an optical energy close to the main photorefractive level of sillenites at 2.2 eV) [15], significant improvement of the recording speed is observed (see Fig. 3(b) and 4(b)). The writing kinetics shows very fast growth with response time of 60 ms for BSO:Ru (50 times faster than the same sample without treatment) and that of 20 ms for BTO:Rh in a diffusion regime. The value of 0.02 s achieved in case of BTO:Rh is among the fastest one for inorganic photorefractive materials reported up to now at 1064 nm and competitive to those reported for polymeric photorefractive composites (in a range of 0.01s to 10 s) [1] and recently proposed $\text{Sn}_2\text{P}_2\text{S}_6:\text{Te}$ crystals [16]. Similar photorefractive response time of 130 ms in a BSO crystal using 810 nm have been reported by Raita et al. [17]. The measured sub-second operation speed is explained by high concentration of stoichiometric defects, in particular by significant amount of Si deficiency, which generates oxygen vacancies. By using green light pre-excitation the charge carriers are excited and fill out the intermediate levels (assuming n-type photoconductivity). We suppose that Rh and Ru addition in sillenite structure introduces trap levels, located closer to the CB (or to the VB) which improves the near infrared sensitivity of the crystals and opens further sensitivity enhancement opportunities by controlling the valence state of Rh and Ru.

2.2 PRLCLV modulation characteristics at near infrared range

The following section present intensity, voltage and time dependence characteristics of BSO:ru and BTO:Rh based PRLCLVs. An example of the probe beam intensity transmitted through the BTO:Rh device as a function of the applied ac voltage is shown at Fig. 3(a). This is a typical characteristics of the PRLCLV device. Next, the phase change is measured by sending the pump and probe beams together to the PRLCLV. The intensity changes of transmitted probe

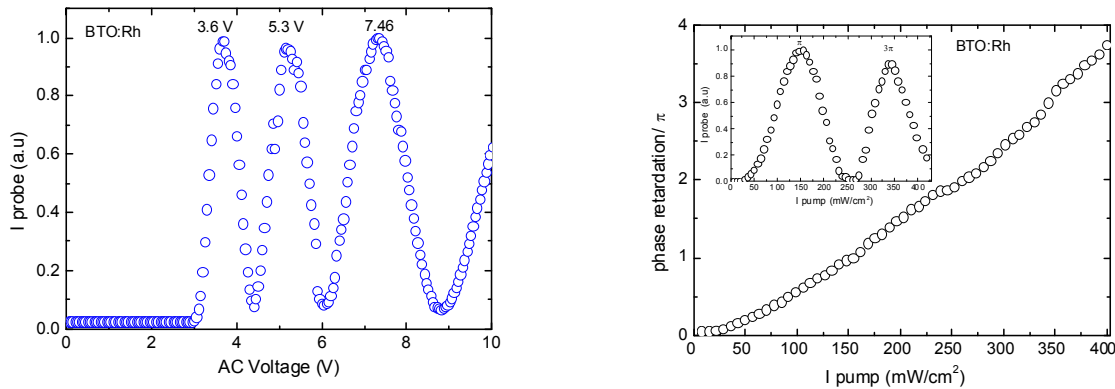


Fig. 3 (a) Normalized probe beam intensity dependence on the applied ac voltage. (b) Phase retardation v.s. pump beam intensity. The applied voltage is 3.6 V at 1 kHz, inset graph-probe beam v.s. pump beam intensity.

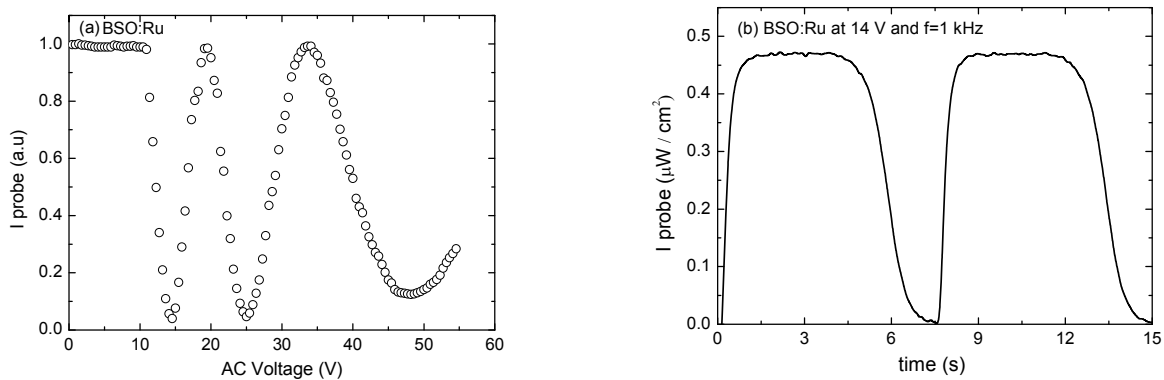


Fig.4 (a) Modulation of the probe beam intensity (a) at different voltages, (b) temporal behavior at a fixed voltage (1-st minima at 14 V) depending on the intensity of the pump light.

beam intensity ($I_{transm.probe}$) at the output of the PRLCLV device by varying the pump intensity (I_p) are shown as inset graph at Fig. 3(b). This dependence allow us to calculate the phase retardation (which is a function of the applied voltage and the pump beam intensity (I_p)) by the formula [18]:

$$\Delta\Phi(I_p) = \frac{2\pi\Delta n(I_p)d}{\lambda} = \sin^{-1} \sqrt{2T(I_p)} \quad (1)$$

where: $T = (I_{transm.probe}/I_{max\ of\ transm.probe})$, d - the LC thickness and $\Delta n = (n_e(I_p) - n_o)$.

Fig. 3(b) shows the phase change behavior of BTO:Rh based PRLCLV device at 1064 nm for the first 4π circles. When the light exposure on the crystal side of the device, BTO:Rh behaves as a light-controlled resistor- due to the crystal's high photoconductivity, it's impedance decreases, which enhances the voltage across the LC layer. This support the LC molecules reorientation and due to the LC strong birefringence at the exit of the valve the light beam obtain a phase retardation Φ for the e - wave and o - wave components. Thus, the reorientation angle of the LC molecules varies from 0 to $\pi/2$, producing a phase shift of several π . The maximum phase retardation of 7.6π will appear when all LCs molecules are aligned along the direction of the applied field.

Figure 4(a) shows similar modulation dependence in case of BSO:Ru based PRLCLV device. As it seen, the behavior is similar to BTO:Rh (Fig. 3(a)), only higher voltage is required to modulate the intensity, due to the larger thickness of the BSO:Ru plate. Figure 4(b) presents the temporal evolution of BSO:Ru PRLCLV device when the 1064 nm pump light is "on" and "off". As it seen, the response time is very fast in a ms range.

Further, an example of an image illumination on PRLCLV device is shown. Figure 5 shows an image illumination of letter "B" when the voltage is at minimal value - positive image (a) and when the voltage is at maximal value - negative image (b). Next, the time evolution of the same image is shown in Fig. 6 (a) at the beginning of the process, (b) at 240 ms and (c) 600 ms. An example of the temporal evolution presented at Fig. 4(b) shows the all optical switching property of our BSO:Ru based PRLCLV device which could be used for further dynamic near-infrared photonic applications.



Fig. 5 (a) Positive (at minimal voltage) and (b) negative (at maximal voltage) image of letter "B" on PRLCLV device.

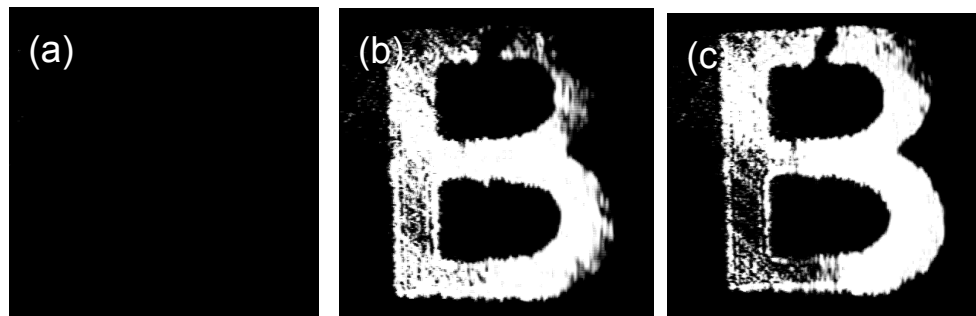


Fig 6. Time evolution of face mask at (a) 0 ms, (b) 240 ms and (c) 600 ms

3. CONCLUSIONS

In summary, we have demonstrated that doping with metals Ru and Rh in sillenite structure could act as very effective dopants, which improves the sensitivity and response speed at the near infrared spectral range. A millisecond response time is measured during real-time holography without any preliminary treatments of the sample. When the crystal is pre-exposed shortly with a green light, the response speed becomes 0.02 s. A possibility to combine sillenite crystal plates with liquid crystal cell into a hybrid organic/inorganic device is demonstrated which opens many perspective for further near infrared applications, where LCs are typically not sensitive.

Acknowledgments: Financial support by NSC, Taiwan under contracts NSC 101-2911-I-009 -508, NSC 101-2221-E-009 -112-MY3 and by Ministry of Education, Taiwan under AUT program is gratefully acknowledged.

The authors are gratefully thankful to the Crystal Growth Laboratory at the Institute of Solid State Physics, Bulgaria for crystal samples growth and preparation.

REFERENCES

- [1] Kober, S., Prauzner, J., Salvador, M., Kooistra, F. B., Hummelen, J. C. and Meerholz K., "1064-nm sensitive organic photorefractive composites," *Adv. Mat.* 22, 1383-1386 (2010).
- [2] Frejlich, J., [Photorefractive materials], Wiley Interscience (2007).
- [3] Caroen, M. G., Mori, M., Gusualdi, M. R. R., Liberti, E. A., Ferrara, E. and Muramatsu M., "Mastication effort study using photorefractive holographic interferometry technique," *J Biomechanics* 43, 680-686 (2010)
- [4] Odoulov, S. G., Shcherbin, K. V. and Shumeljuk A. N., "Photorefractive recording in BTO in the near infrared," *J. Opt. Soc. Am. B* 11, 1780-1785 (1994).
- [5] Barbosa, E. A., "Holographic imaging with multimode, large free spectral range lasers in photorefractive sillenite crystals," *Appl. Phys. B.* 80, 345-350 (2005).
- [6] Marinova, V., Lin, S. H., Sainov, V., Gospodinov, M. and Hsu K. Y., "Light-induced properties of Ru-doped $\text{Bi}_{12}\text{TiO}_{20}$ crystals," *J. Optics A: Pure and Applied Optics* 5, S500- S506 (2003).
- [7] Marinova, V., Liu R. C., Lin S. H. and Hsu K.Y. "Real-time holography in ruthenium doped bismuth sillenite crystals at 1064 nm" *Opt. Lett.* 36, 1981-1983 (2011).
- [8] Marinova, V., Liu, R. C., Lin, S.H., Chen, M.S., Lin, Y. H. and Hsu K. Y., "Near infrared properties of Rh-doped $\text{Bi}_{12}\text{TiO}_{20}$ crystals for photonic applications," *Opt. Lett.*, 38 , 495-497 (2013)
- [9] Brito, I. V., Mori, M., Gesualdi, M. R. R., Ricardo, J., Palacios, F., Muramatsu, M. and Valin J. L., "Photorefractive digital holographic microscopy applied in microstructures analysis," *Opt. Commun.* 286, 103-110 (2013)
- [10] Aubourg, P., Huignard, J. P., Hareng, M. and Mullen R. A., "Liquid crystal light valve using bulk monocrystalline $\text{Bi}_{12}\text{SiO}_{20}$ as the photoconductive material," *Appl. Optics* 21, 3706-3712 (1982).
- [11] Bortolozzo, U., Residori, S. and Huignard, J. P., "Nonlinear optical applications of photorefractive liquid crystal light valves," *Journal of Nonlinear Optical Physics & Materials* 16, 231-236 (2007).
- [12] Bortolozzo, U., Residori, S. and Huignard, J. P., "Adaptive holography in liquid crystal light valves," *Materials* 5, 1546-1559 (2012).
- [13] Bortolozzo, U., Residori, S. and Huignard J. P., "Beam coupling in photorefractive liquid crystal light valves," *J. Phys. D* 41, 224007 (2008).
- [14] Sveshtarov, P. and Gospodinov M., "The effect of the interface shape on automatic Czochralski weight diameter control system performance" *J. Cryst. Growth* 113, 186-208 (1991).
- [15] Oberschmid, R., "Photoconductive and photorefractive effects in BSO," *Phys. Stat. Solidi A* 89, 263-270 (1985).
- [16] Bach, T., Jazbinšek, M., Montemezzani, G., Günter, P., Grabar, A. A. and Vysochanskii Y. M., "Tailoring of infrared photorefractive properties of $\text{Sn}_2\text{P}_2\text{S}_6$ crystals by Te and Sb doping," *J. Opt. Soc. Am. B* 24, 1535-1541 (2007)
- [17] Raita, E., Kobozev, O., Kamshilin, A. A. and Prokofiev V. V., "Fast photorefractive response in $\text{Bi}_{12}\text{SiO}_{20}$ in the near infrared," *Opt. Lett.* 25, 1261-1263 (2000).
- [18] Yeh, P. and Gu C., [Optics of liquid crystal display], Wiley Interscience (1999).